Enhancing Parameters Estimation in Subsurface Imaging with Ground Penetrating Radars

Deepak Pareek[a] and Jyoti Khandelwal[b]
Department of CSE, University of Engineering and Management, Jaipur, India

Keywords: GPR, U-net, HMC, Convolution, Regression.

Abstract: Ground Penetrating Radar (GPR) images cannot be directly inverted to obtain subsurface source images, making it a challenging computational problem. This work investigates two fundamentally different approaches to solving the GPR inverse problem: a Hamiltonian Monte Carlo (HMC) method and a U-net neural network. HMC, a Markov Chain Monte Carlo technique, evolves the system state to minimize the objective function, while U-net leverages convolutional neural networks for regression to predict pixel-wise reflectivity values. Extensive experiments on simulated GPR data with varying numbers of sources reveal that HMC's performance, measured by the Structural Similarity Index (SSI), deteriorates as more sources are introduced. In contrast, the U-net model demonstrates remarkable robustness, maintaining high SSI scores even with numerous sources present. The results indicate that in scenarios with abundant GPR training data and complex source distributions, a U-net model is preferable over HMC due to its superior generalization capability and efficient parallel processing. However, HMC offers interpretability advantages by allowing statistical analysis of individual pixels. This work highlights the trade-offs between the two approaches and provides insights for selecting the appropriate method based on the problem's complexity and data availability.

1 INTRODUCTION

1.1 Ground Penetrating Radar

GPR Fig. 1 is broken down into the below subcategories, which are categorized as geophysical surveys and specifically involve the use of radar to probe the surface of the ground. This method is very helpful for locating items on the ground, especially utility lines, where the gourd contains features like concrete, metal, or plastic lines, cables and even masonry structures. GPR works by emitting high-frequency electromagnetic pulses into the earth's surface and measuring the reflection of the pulse that comes back from the objects and interfaces lying in the ground. In this study we use two methods to obtain object source images from GPR images: Hamiltonian Monte Carlo and a U-net Neural Network.

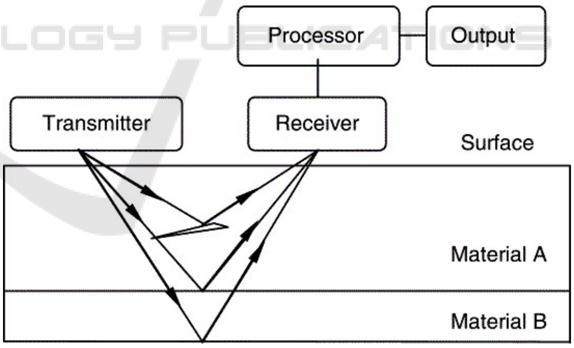

Figure 1: GPR System.

1.2 Hamiltonian Monte Carlo

Markov Chain Monte Carlo (MCMC) methods are widely used to obtain source images from GPR results. For instance (Hunziker et al., 2019) (Qin et al., 2016) use Bayesian-based MCMC methods to simulate and reconstruct GPR source images. In this work, we use a Hamiltonian Monte Carlo approach (HMC) to do this task. HMC was initially developed in 1987 by (Duane et al., 1987) as a method based on the idea of energy conservation and minimal action path from Hamiltonian Mechanics (HM).

[a] https://orcid.org/0009-0009-7739-1832
[b] https://orcid.org/0000-0002-3027-258X

Khandelwal, J. and Pareek, D.
Enhancing Parameters Estimation in Subsurface Imaging with Ground Penetrating Radars.
DOI: 10.5220/0013263400004646

In *Proceedings of the 1st International Conference on Cognitive & Cloud Computing (IC3Com 2024)*, pages 154-160
ISBN: 978-989-758-739-9

Compared to standard random walk-in metropolis algorithms, HM properties allow HMC methods better convergence to the typical set-in problems with high dimensionality. This is therefore very useful for GPR problems where the solution space has the same dimensions as the number of pixels in the image (therefore for typical images of 64×64 pixels one has to consider systems of dimensions up to 4096)

1.3 Neural Networks

The U-net fig. 2 architecture, initially developed for segmenting biomedical images, consists of two main components: it contains an encoder and a decoder, an encoder and a decoder. In semantic segmentation, unlike in image classification applications where the main output is the primary goal, pixel-level accuracy is needed, and a way to transfer the detected features when they are processed at different encoder stages back to the pixel domain is required (Ronneberger et al., 2015). The encoder part of the U-net structure, depicted in Fig. 1, usually employs an existing classification network like VGG or ResNet (He et al., 2015). This component uses a layer of convolution block made up of several numbers of convolutions each of which is followed by down sampling max pooling to extract multi-level features from the input image. The decoder, which forms the second half of the U-net, should be able to generate an output map that is high in resolution and semantic content from a set of lower-resolution features obtained by the encoder section. This process involves; upsampling operations on the feature maps; concatenation of features; and more convolutional operations to obtain per-pixel density maps.

2 METHODOLOGY

In this section, we explain our approach to solve the GPR problem using HMC and Neural Network.

2.1 Selecting a Temp

To generate our GPR data we have used a forward model simulation. The usual procedure for GPR image reconstruction involves performing time evolution of a simulated source using Finite Time Difference Methods (FDTD) to simulate wave propagation for a candidate source distribution. Although more efficient approaches using other methods such as Runge-Kutta schemes, (WAN, 2020) have been developed, these methods are often time-consuming and resource-intensive. Therefore, in this study, we use a

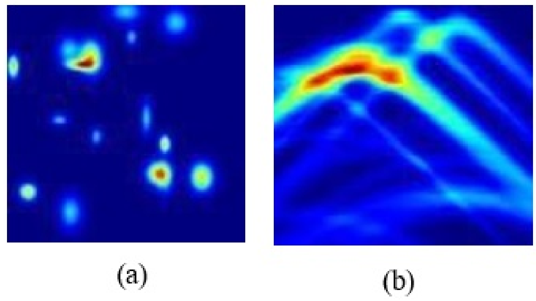

Figure 2: GPR image, (a) Forward model obtained from Object Image (b) Object Image.

simplified method based on simple wave propagation equations to build a forward model, that is, a simulation of the resulting GPR image produced by a proposed source. The resulting forward image will be modelled by the equation (1).

$$A(r) = A_0 P(2\Delta t) e^{-} 2\gamma r \tag{1}$$

Where γ is a dampening constant depending on the media properties, r is the Euclidean distance from the GPR to each source and DT = r /u, where u is the speed of light in the media, is the time taken to travel from the GPR to the source. In the equation above, the reader will recognize the typical equation of an over-damped harmonic oscillator (hyperbolic equations). This is the result of considering only the evolution of the amplitude of the wave with time and omitting all the imaginary terms that result in more complicated interactions like destructive interference. Other usual effects in this field like refraction caused by water droplets in the media have also been omitted here and introduced in a simplified way in the source model as Gaussian noise. The equation above can be rewritten as propagator equation D = G · F where F is the pixel-wise map of sources, G is the wave propagator given by A(r) and D is the resulting image in the GPR. We call the resulting image forward model as shown in Fig 2 (a) and (b).

2.2 Hamiltonian Monte Carlo

Details of the Hamiltonian Monte Carlo method can be found in (Betancourt, 2018). As usual, our Hamiltonian is the resulting sum of potential and kinetic energy functions, where kinetic energy is independent of spatial coordinates and potential energy is independent of momentum coordinates 1. Momentum values are generated pixel-wise with random normal distribution, with a standard deviation dependent on the temperature of the system. The kinetic energy is then calculated as the classical kinetic energy considering the identity as a mass matrix, therefore,

$K(p_{)} = 1/2pp2$. The potential function is our objective function and it is through the gradient of the potential that our state converges to the typical set. The potential energy is calculated as the squared error $V(q) = 1/2(DGF)2$ where D is the real forward image, G is the propagator of the problem as described above, and F is the current state of the HMC chain. At each iteration, a new Hamiltonian resulting from new kinetic and potential energies is calculated. The resulting Hamiltonian evolves in time with the leapfrog integration method.

For $0 \leq n < \frac{T}{E}$ do

$$A \leftarrow A - E\,\delta V(q_{n+\frac{1}{2}})\,\delta q_n$$

$$q_{n+1} \leftarrow q_n + E p_{n+\frac{1}{2}}$$

$$A_{n+\frac{1}{2}} \leftarrow A_{n+\frac{1}{2}} - 2\,\delta q\,(a_n + q)$$

End For.

Where T is the total time evolved and E is the step size. This simple method allows us to evolve the Hamiltonian in time following a path that minimizes its action, as described by Hamilton equations. Note that if K and V are scleronomic, Hamilton equations reduce to

$$\frac{dq}{dt} = \frac{\delta K(p)}{\delta p} \tag{2}$$

$$\frac{dp}{dt} = \frac{\delta V(q)}{\delta q} \tag{3}$$

Which bears similarity to the leapfrog algorithm. The forward image used for the HMC method was of size 64 × 64 and was generated using the forward model described above for 1, 3 and 50 sources. The simplified single-source scenario was used to build and tune hyperparameters for the HMC model. Hyperparameters in HMC govern the evolution of the state and its convergence to the typical set. These parameters are typically referred to as Temperature and step size, where the former governs the amount of chaos or variation introduced to the system at each iteration, and the latter is the step size used in the leapfrog integrator to calculate the variation of the Hamiltonian at each integration step. One of the difficulties of the HMC method is to use optimal parameters for convergence, which depend on the typical set and the nature of the problem. In addition to the ones described above, it is also useful to find a good seed to allow for faster convergence. To find the best values for these parameters (T, step size, seed) an exhaustive search over common parameter ranges was conducted in the iris-cluster (Varrette et al., 2014). After finding the best set of parameters, we run the HMC for 10,000 iterations for 1, 3 and 50 initial sources. To compare the final states to the initial simulation we perform a structural similarity test on the final states smoothed with a Gaussian filter. For completeness, we also compare the initial simulation and the final HMC state with a full waveform inversion model obtained using back projection.

2.3 Neural Networks approach

As we see the in GPR data (see Fig. 2 & 3) every pixel intensity defines the reflectivity and shows the object property. It means we have to predict the exact values of these pixels to find the objects. Traditionally U-net is used for segmentation and assigns class labels to each pixel. But in our case, it is more of a regression problem to predict the reflectivity values of pixels.

- Neural Networks Architecture: The network architecture, inspired by U-net as illustrated in Fig. 1, consists of two main pathways: PATH A has elements that compress, control or confine: regressive, directive and enclosed (left side of the figure), PATH B has elements that open up, encourage, and set free: progressive, persuasive and most encompassing (right side of the figure). The compressive path is implemented with the general architecture of a convolutional network. It successively performs two convolutions of 3x3 with the same padding and uses the ReLU activation function; and then a max pooling of 2x2 with a stride of 2 for down sampling. Thus, in the down-sampling processes, the number of channels is doubled while the size of the feature maps is reduced. Steps of the expansive path are upsampling the feature map, then followed by a convolution operation with a 2 x 2 filter, which is also known as up-convolution that reduces the number of channels in the feature map by two at that step. Which is then concatenated to a feature map extracted from the compressive path at the same level but with precise cropping. Two 3 x 3 convolutions and ReLU are next to each other, one convolution is followed by ReLU. The cropping is needed because the convolution operation crops out a portion of the border in each instance of the feature map. The network ends with a 1x1 convolution layer at the last stage that transforms each 64-element vector into the output. Blue rectangles denote the multi-channel feature maps. Next to each rectangular figure, there is a number that represents the number of channels; the x-y dimensions are also provided in the lower left corner. White rectangles are the duplicative feature maps as indicated below. Some of the operations are

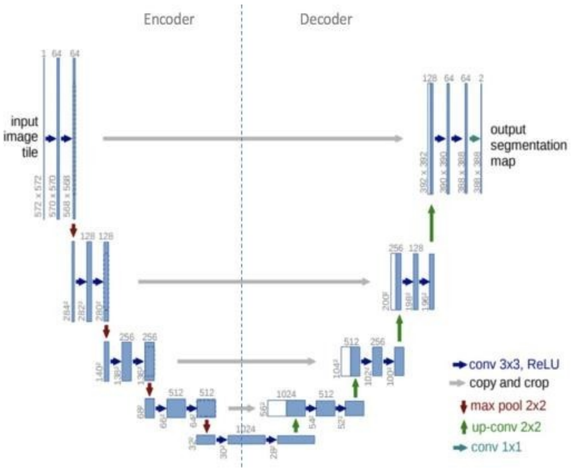

Figure 3: U-net architecture (example for 32x32 pixels in the lowest resolution).

shown by the arrows linking these elements.

- Training: The input to the model is, image pairs consisting of the input image and the object map of the same image. Indeed we use stochastic gradient descent for the training implementation. The input images underlying our filters are of the dimension 128 x 128 pixels. For better detail capturing, the batch size is selected to be 32 and the learning rate is 1e-4. As for the loss function, since our objective is less about trying to categorize data as it is to predict it, we use Mean Squared Error (MSE). It also enables this choice to make the pixel intensities forecasts more accurate. To effectively capture these intensity values, we implement the ReLU function as our non-linear activation. We have also added dropouts 0.4 to stop overfit.

$$\mathrm{MSE} = L_D(x_i - y_i)^2 \tag{4}$$

- Data Augmentation: It is necessary to build an appropriate level of invariance and robustness in the network by applying the strategies of data augmentation. We used the augmentations library for this and added Gaussian noise to the data to make it robust (Fig. 4).

3 RESULTS

In this section, we discuss our results from HMC and Neural Network approach.

3.1 HMC

The final state (object image) from the resulting HMC chain is shown for 1, 3 and 50 sources in Fig. 5 to 7 respectively. The resulting forward image of the final HMC state and the real image for the same sources are shown in Figures 5 to 10. Table 1 shows the values of SSI for all sources for both the HMC result and backpropagation.

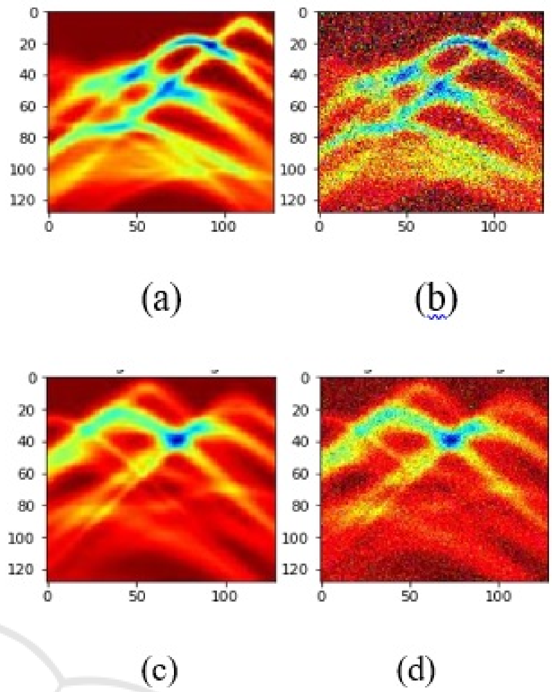

Figure 4: Gaussian Noise Augmentation, (a) and (c) represent the Original image, (b) and (d) represent the Augmented Image.

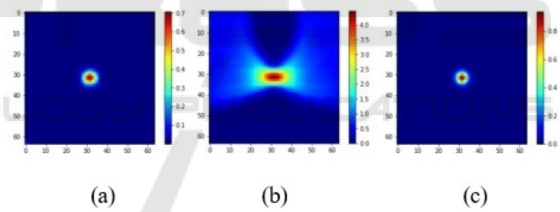

Figure 5: Left to right for 1 source, (a) Final state of the HMC chain (b) source image obtained with backpropagation (c) real (simulated) source image

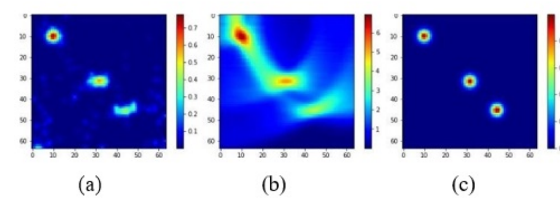

Figure 6: Left to right for 3 sources (a) Final state of the HMC chain (b) source image obtained with backpropagation (c) real (simulated) source image

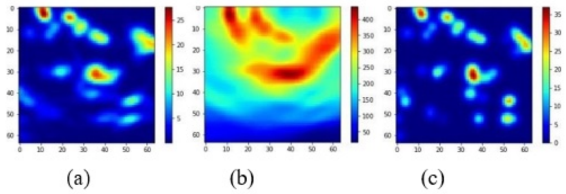

Figure 7: Left to right for 50 sources: (a) Final state of the HMC chain (b) source image obtained with backpropagation (c) real (simulated) source image

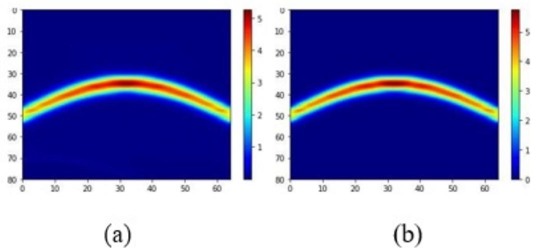

Figure 8: From left to right for 1 source, (a) the forward image of the HMC final state and (b) the forward image of the real source image

Table 1: SSI values for deferent numbers of sources.

Sources	HMC	Backpropagation
1	0.99	0.31
3	0.84	0.05
50	0.52	0.006

3.1.1 Neural Network

Table 2, shows the results from neural network predictions. We used the Multi-Scale Structural Similarity Index (MSSIM) and Structural Similarity Index (SSIM) to compare matrices (Higher values are better). The table presents the mean values of the Multi-Scale Structural Similarity Index (MSSIM) and Structural Similarity Index (SSIM) achieved by the U-net model on the test data. These metrics quantify how similar the U-net's predicted object images are to the ground truth images, with higher values indicating better structural similarity and, consequently, better performance.

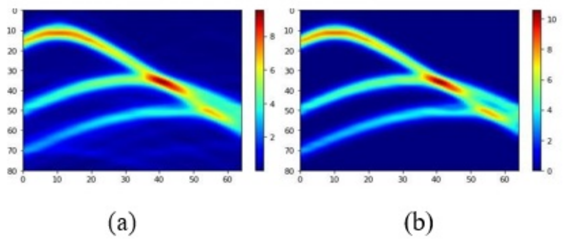

Figure 9: From left to right for 3 sources: forward image of the HMC final state, forward image of the real source image

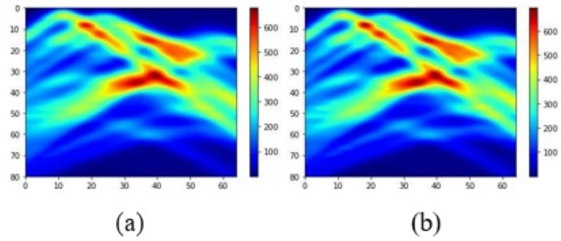

Figure 10: From left to right for 50 sources: forward image of the HMC final state, forward image of the real source image

Table 2: Prediction result.

Label	Prediction	SSIM	MSSIM
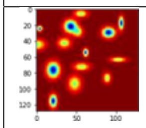	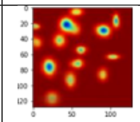	0.99	0.94
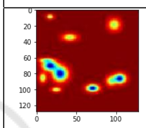	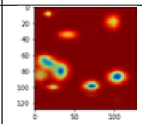	0.99	0.95
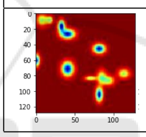	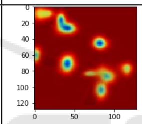	0.99	0.95

Table 3: Shows the mean values of SSIM and MSSIM on test data.

Test data number	Mean SSIM	Mean MSSIM
1000	0.99	0.93

The purpose of Table 3, is two-fold: first, it evaluates the generalization performance of the trained U-net model by reporting its mean SSIM and MSSIM scores on a separate test dataset of 1000 samples. This demonstrates the model's ability to perform well on unseen GPR data. Second, it provides a direct comparison point with the HMC results reported in Table I, allowing the reader to appreciate the relative strengths of the U-net approach, especially in scenarios with many sources where the HMC method's performance declines.

Likewise, from the results presented in Table III that demonstrate high mean SSIM and MSSIM on the test data, confidence can be gained with the proposed U-net for subsurface imaging with GPR data. It supports the authors' assertion that the U-net model is more suitable for handling several sources of complexity in the capturing of data than the HMC technique. In general, Table III is instrumental in measuring the generalization capability of the U-net model and provides valuable insight into this study; it underscores the U-net model's capacity to obtain highly accurate results in detecting subsurface sources in unseen data.

4 COMPUTATIONAL COST ANALYSIS

However, besides the comparison of the performance, the computational costs of the HMC and U-net should be compared as well, since they play a critical role in determining the feasibility of these approaches' application in practice.

4.1 Time Complexity

The Hamiltonian Monte Carlo (HMC) is an iterative sampling tactic, and the time-consuming option increases with the number of iterations needed to reach convergence. Further, due to the high dimensions induced by the number of pixels in the GPR image, HMC's time complexity becomes high. On the other hand, the U-net neural network approach once trained can predict in a single forward pass and hence the time complexity will be constant irrespective of the input size/complexity.

4.2 Resource Requirements

Dew Fletcher indeed pointed out that HMC is a computationally dense method, especially for problems with high dimensionality. Depending on the size of the objective function and the number of parameters there can be a high computational cost, computations of the objective function and its gradients are needed in each iteration which may be expensive and can require parallel computing resources or special purpose hardware acceleration.

On the other hand, the U-net model even though it may be time-consuming during training, can take advantage of the parallelism that modern GPU offers for inference. The evaluation of the model shows that it can construct a prediction system based on the new data with relatively low overhead helping to reduce the computational load and increase the efficiency of the solution for deployment.

4.3 Practical Implications

Therefore, near real-time predictions are mandatory, such as in real-life applications of GPR, the constant time complexity and the insignificant inference overhead of the U-net model seem to be concomitantly beneficial. Also, it is crucial to note that the actualization of the model requires flexibility in the choice of deployment mechanism.When the trained U-net model is concluded on resource limited devices or edge computing platforms, it makes the model very suitable for use.

However, for situations where the distinction between different categories is important or the results need to be presented and analyzed statistically the HMC method may seem preferable. Covariance and the ability to follow the Markov Chain means that the changes in each pixel and the statistical properties in the image such as the value distribution can be analyzed and this could prove useful in research and analysis oriented applications.

However, it is necessary to emphasize that when choosing between computational cost and accuracy, one should think more about the special conditions of the particular application. In cases where there is ample computation to be done and where exact solutions are desired the HMC method could be used though it has been mentioned to be computationally more expensive. On the other hand, where information is in limited supply or time is critical and near real time predictions are necessary then perhaps the U-net model despite having slightly less interpretability may be more beneficial.

5 CONCLUSION

It can be observed that the usage of U-net NN has enhanced the results as compared to HMC. This improvement however is not without a downside since Unet requires a large amount of data to train the model and HMC does not. HMC also enables tracking the changes in each single pixel through the Markov Chain thus enabling statistical calculation such as variance and value distribution for each single pixel, which Unet does not enable because it was undefined. Further investigations might attempt to use a hybrid method combining both techniques, as well as a more complex forward model with interactions between wavefronts and more dispersion effects with the underground media.

REFERENCES

(2020). An interpolating scaling functions method with low-storage five-stage fourth-order explicit runge-kutta schemes for 3d ground penetrating radar simulation. *Journal of Applied Geophysics*, 180:104128.

Betancourt, M. (2018). A conceptual introduction to hamiltonian monte carlo.

Duane, S., Kennedy, A., Pendleton, B. J., and Roweth,

D. (1987). Hybrid monte carlo. *Physics Letters B*, 195(2):216–222.

He, K., Zhang, X., Ren, S., and Sun, J. (2015). Deep residual learning for image recognition.

Hunziker, J., Laloy, E., and Linde, N. (2019). Bayesian full-waveform tomography with application to crosshole ground penetrating radar data. *Geophysical Journal International*, 218(2):913–931.

Qin, H., Xie, X., Vrugt, J. A., Zeng, K., and Hong, G. (2016). Underground structure defect detection and reconstruction using crosshole gpr and bayesian waveform inversion. *Automation in Construction*, 68:156–169.

Ronneberger, O., Fischer, P., and Brox, T. (2015). U-net: Convolutional networks for biomedical image segmentation. *arXiv e-prints*, page arXiv:1505.04597.

Varrette, S., Bouvry, P., Cartiaux, H., and Georgatos, F. (2014). Management of an academic hpc cluster: The ul experience. In *2014 International Conference on High Performance Computing Simulation (HPCS)*, pages 959–967.